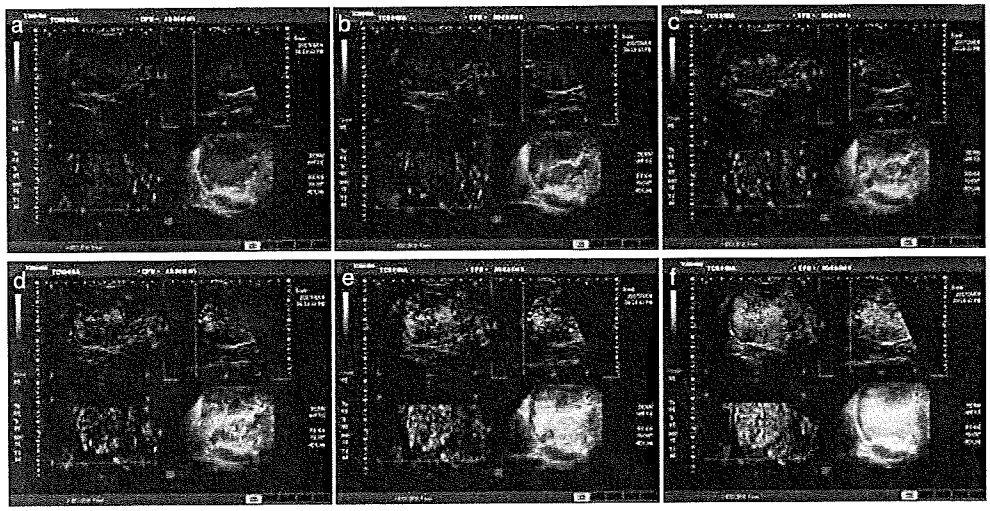

図4　肝血管腫の造影4D-US(MPR表示)
a～f は時間経過を示し，それぞれ上段は左がA面，右がB面，下段は左がC面で，右はMIP．周囲より血流が流入していく様子が観察できた．

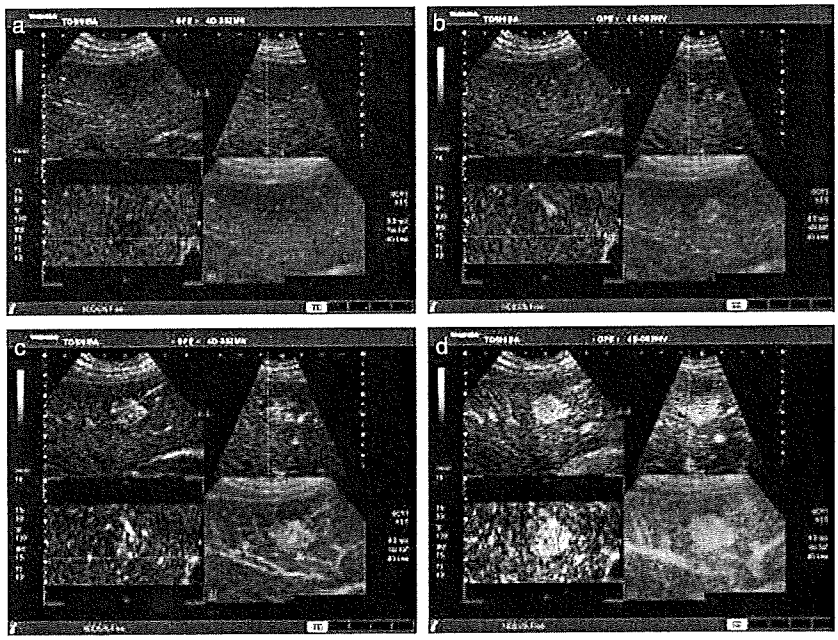

図5　肝細胞癌の造影4D-US(MPR表示)
a～d は時間経過を示す．右下のMIP像をみると，右下から血流が流入し，右上に流出している門脈と考えられ像が観察された．

造影モードは3.5 MHzで行った．超音波造影剤はソナゾイド®を用い，造影超音波のときはmechanical index(MI)値を0.20～0.30とした．造影モードはLow MI Contrast Harmonic Imagingを用いた．

肝疾患において4D-USおよび造影4D-USを行い，造影4D-USによる診断，4D-USガイドによるRFA穿刺，RFAの治療モニター，RFAの効果判定について検討した．4D-USの表示方法は，通常の断面をA面とし，それに直行する2面をそれぞれBおよびC面として示すMPR表示を用いた(図1)．

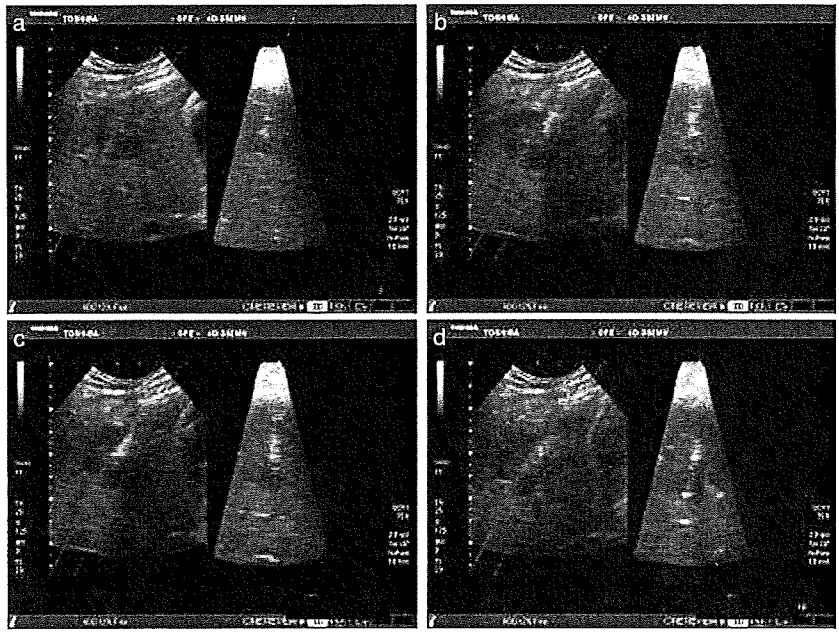

図6　肝細胞癌のラジオ波焼灼療法(RFA)穿刺時の4D-US(VolPure表示)
a～dは時間経過を示す．肝細胞癌の中心にRITA針が穿刺され，展開される様子が2方向から観察された．

MPR表示のとき4分割された画面の右下はA面のmaximum intensity projection(MIP)を表示した．また，RFAの穿刺時などはVolPure表示とし，左の面をA面，右をA面に直交し，穿刺ラインを含む面のMIP像とした(図2)．

症例呈示

1．肝膿瘍の診断

Bモードでは辺縁はやや低エコーでな産に無エコーの腔が認められた．ソナゾイド®で造影4D超音波を行うと，腔の周囲はおよび境界に多血流の部分が観察され，内部に腫瘍を示す結節は認められず，肝膿瘍と診断した(図3)．

2．肝血管腫の診断

Bモードでは肝右葉に約7 cmの境界やや高エコーの低エコー腫瘍が認められた．これに対し造影4D-USを施行した．時間経過とともに造影態度を多方向から観察できた．まず，周囲の流入血管が観察され，その後，腫瘍は周囲よりゆっくり造影されていき，内部の血管は微細で，明らかな悪性腫瘍を考える異常血管は認められず，肝血管腫と診断した(図4)．

3．肝細胞癌の診断

Bモードでは肝S5に約2 cmの低エコー腫瘍が認められた．これに対し造影4D-USを施行した．MIP像でわかりやすいと考えられるが，まず腫瘍に流入する肝動脈が描出され，その後腫瘍は全体が急速に濃染し，流出血管も描出された(図5)．造影剤投与より10分後の実質相では肝腫瘍にソナゾイド®の残存はほとんど認められず，肝細胞癌と診断した．

この症例は肝細胞癌が単発であったため，RFAを施行した．RFAにはVolPureで観察し，穿刺を施行すると，肝細胞癌の中央に穿刺針が刺入され，展開が肝細胞癌の周囲まで広がっていることが2方向から確認することができ，穿刺および展開が正確にされていることが確認できた(図6)．焼灼を4D-USで観察すると，展開針の先端から高エコーの領域が広がり，肝細胞癌のあった領域を超えて拡大していく様子が多方向から確認できた(図7)．

翌日，治療した領域の造影4D-USを施行した．肝細胞癌の残存を示す染影は認められず，肝細胞癌は十分焼灼されていたことが多方向から確認できた(図8)．

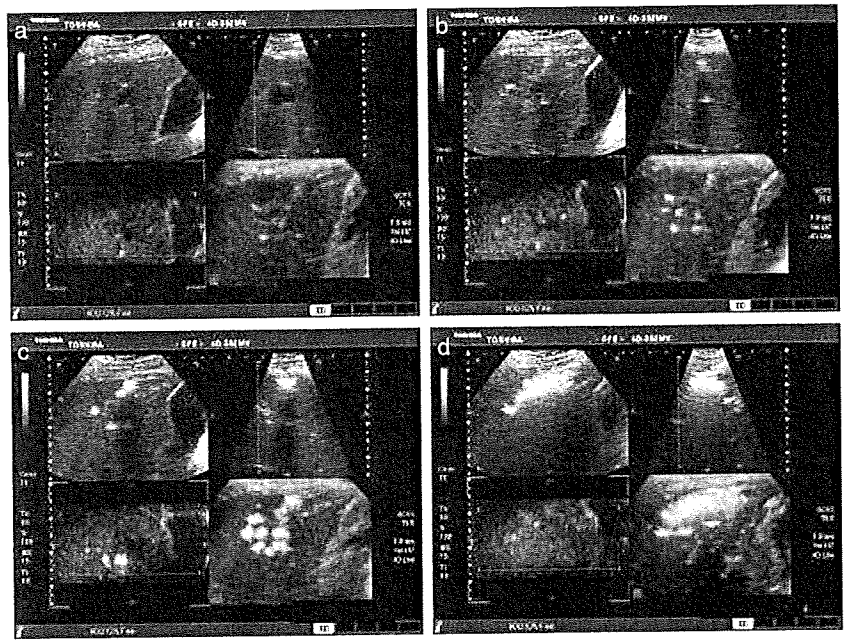

図7　肝細胞癌のラジオ波焼灼療法(RFA)焼灼時の4D-US(MPR表示)
a～dは時間経過を示す．肝細胞癌の焼灼される様子が詳細に観察された．

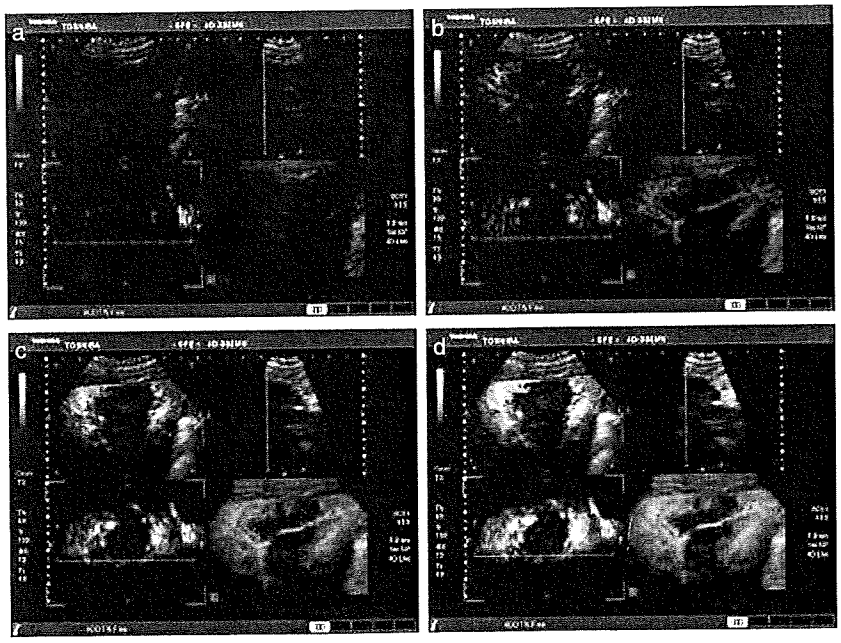

図8　ラジオ波焼灼療法(RFA)後1日の肝細胞癌の造影4D-US(MPR表示)
a～dは時間経過を示す．RFAにより肝細胞癌が十分焼灼されている様子が観察された．

考　察

4D-USおよび造影4D-USにより，肝腫瘍を3次元的に診断することが可能となり，MPRなどで観察することにより，多方向から詳細に肝腫瘍や周囲の構造を観察，診断することが可能となった．

また，RFAにおいて，今までの断層像では左右方向のズレは容易に観察することができたが，これと直交する前後方向のズレを確認することは難しかったが，穿刺に4D-USを用いることにより，前後方向のズレまで容易に確認することができ，正確な穿刺ができ，RFAの治療効果に寄与することが考えられた．

RFAの効果判定では多方向から焼灼域を観察することができ，効果を判定することが可能であった．

現在，周囲の脈管や臓器の構造をもとに，RFAの術前，術中，術後のボリュームデータをもとに，3Dまたは4D-USの位置を合わせるソフトウェアが開発されてきている．これにより位置あわせを正確に行うことができれば，造影エコーのみで正確なRFAの治療，効果判定が可能となる．

文　献

1) 山田昌彦，森安史典．今考えられる造影超音波の役立て方と将来の展望．写真とシェーマでみえる！腹部エコー－適切な診断のための走査と描出のコツ－．住野泰清・編．東京：羊土社；2007．p. 212-9.
2) 飯島尋子．ソナゾイドの投与法，装置・撮像条件，自相．Innervision 2007；22：8-10.
3) 山田昌彦．造影3D・4D超音波診断．Innervision 2007；22：53-6.

*　　*　　*

J. Tokyo Med. Univ., 67(2): 169–175, 2009

Phagocytosis of Ultrasound Contrast Agents and Diagnostic Low Intensity Insonation Increased the Expression of Heat Shock Protein 70 in Kupffer cells

Munire REXIATI, Tomihiko HIROKAWA, GuangJian LIU, Fuminori MORIYASU

Fourth Department of Internal Medicine, Tokyo Medical University

Abstract

Purpose

Phagocytizing ultrasound contrast agents by Kupffer cells, which are liver macrophages, enhances clinical diagnostic ability in ultrasound screening for liver tumors. The bioeffects of insonation on the phagocytized ultrasound contrast agent are still not well known. We evaluated the cell stress in this kind of ultrasound examination from diverse aspects.

Methods

We used the ultrasound contrast agent (Sonazoid) in this study. Kupffer cells from 60 rat livers were cultured and assigned randomly to 2 groups. One group was insonated only (US). The other group was insonated after the Kupffer cells phagocytized the Sonazoid microbubbles. Each group was divided into 4 subgroups according to intensity of insonation as follows, mechanical index (MI) 0.2 ($n=8$), 0.6 ($n=8$), 1.6 ($n=8$), and control ($n=6$). Insonation was applied for 30 seconds by clinical ultrasound diagnostic equipment (Aplio, Toshiba). Microscopic observation was performed before and after insonation to detect morphological change. The production of heat shock protein 70 (HSP70) and leakage of lactase dehydrogenase (LDH) were determined to evaluate the cell injury.

Results

In both groups, no significant morphologic changes of microbubbles were observed at MI 0.2, while burst and vanishing of the microbubbles were observed at MI 1.6. There were no obviously morphologic changes of Kupffer cells in all groups. In the expression of HSP70, no significant change was observed in the US group, however in the CEUS group, expression significantly increase at MI 0.2 ($p<0.05$) compared with controls. Intergroup comparisons at the same ultrasound intensity level, the expression of HSP70 in the CEUS group was significantly stronger ($p<0.05$) than other groups especially at MI 0.2. The leakage of LDH did not significantly differ among any groups.

Conclusion

This study showed that insonation after Kupffer cells phagocytosed the ultrasound contrast agent caused no morphologic change in Kupffer cells. However it is undeniable that cell-stress could be increased.

Received September 3, 2008, Accepted December 25, 2008

Key words: Kupffer cell, HSP, Perflubutane, Ultrasound

Corresponding author: Fuminori MORIYASU, Chairman & Professor, Department of Gastroenterology and Hepatology, Tokyo Medical University, 6-7-1 Nishi-Shinjuku, Shinjuku-ku, Tokyo 160-0023

TEL: +81-3-5325-6838, FAX: +81-3-5325-6840; E-mail: moriyasu@tokyo-med.ac.jp

Introduction

Studies have shown that ultrasound (US) contrast agents improve the ability of US examinations to detect hepatocellular carcinoma. It is assumed that the US perflubutane microbubble (Sonazoid™) contrast agent is especially helpful for both liver vascular imaging because of it is activity and also liver parenchyma imaging (Kupffer imaging) by enhancing the contrast of the HCC and metastasis lesions greater degree than other previous ultrasound contrast agents due to the phagocytization perflubutane bubbles in Kupffer cells[1]. However there is concern that the destruction and oscillation of phagocytosis of bubbles during insonation may affect the function and viability of Kupffer cells. A previous paper reported some hepatic cell damage after destruction of microbubbles[2]. In this study, we attempted to observe morphological changes of Kupffer cells and increased HSP 70 expression in vitro after insonation using a clinical ultrasound scanner.

Materials and Methods

Animals

Male Wistar rats aged 18 weeks and weighing 300–400 g were purchased from CLEA Japan Inc. (Tokyo, Japan). All experimental procedures were performed in accordance with experimental protocols approved by the Animal Ethical Committee of Tokyo Medical University.

Kupffer cell isolation

Rat Kupffer cells were isolated. The isolation method was similar to that report in a previous paper described[3]. Anesthesia was performed by intraperitoneal injection of pentobarbital sodium (50 mg/kg, Dainippon Sumitomo Pharma Co., Ltd., Osaka, Japan) in all animals. In all rats after a median line incision the portal vein was exteriorized and catheterized with an indwelling catheter. The venae cavae were also exteriorized and ligated. Rat livers were perfused by indwelling catheters in situ with calcium-free minimum essential medium (Sigma, St Louis, USA), followed by 0.3% pronase (Roche Diagnostics Corp., Indianapolis, IN, USA) and 0.025% type IV collagenase (Sigma) in Dulbecco's modified Eagle's medium/F-12 (Sigma). After preparation the livers were carefully removed and minced. The suspension containing Kupffer cells was incubated with 0.035% pronase and 62.5 units/mL DNase (Sigma) in Dulbecco's modified Eagle's medium/F-12 in a shaken water bath at 37 C for 20 min. After being centrifuged several times, Kupffer cells were separated and incubated for 48 hours before the experiment.

Ultrasound Contrast Agent

Perflubutane (Sonazoid™; Daiichi Sankyo Company Ltd., Tokyo, Japan), consisting of stabilized gas microbubbles 2–3 μm in diameter in aqueous suspension, was used as the ultrasound contrast agent in all experiments.

Microscopic Observation of Ultrasound Contrast Agent Phagocytosis

We evaluate morphological changes in Kupffer cells by microscopy. Kupffer cell phagocytosis of microbubbles was observed under a microscope (IX70, Olympus, Tokyo, Japan) and recorded by a camera (model JU-TU531T, Toshiba Corp., Tokyo, Japan). The small glass plate on which Kupffer cells had been cultured was inverted them placed into another large culture well with 40 ml culture medium. We added 0.5 ml contrast agent at 1/1000 standard concentration under the small glass plates using a 21 G needle. Then the bubbles of perflubutane settled near the Kupffer cells. Six cells were selected at random and recorded by video during the phagocytosis. The 6 cells were photographed before and after insonation of each MI.

Insonation

Insonation was performed with an SSA-770A system (Aplio : Toshiba Medical Systems Co, Ltd, Tokyo, Japan) set on a conventional B mode with a PTV-382M probe, a small convex-shape probe that transmitted and received center frequencies of 3.5 MHz. The insonation conditions were as follows : frame rate 15 frames/sec, duration of insonation 30 sec, single focus, on the bottom of the culture dish containing the Kupffer cells.

Three levels of MI were selected for insonation in the experiments as follows : no insonation, MI 0.2, MI 0.6, and MI 1.6, because MI 0.2 is popular for low MI imaging. MI 1.6 is the maximum intensity of the ultrasound system and MI 0.6 is the midpoint. The MI is useful as an index of acoustic intensity, defined as the maximal acoustic negative pressure on the ultrasound field, divided by the square root of the central transmitted frequency.

Kupffer cells from 60 rat livers were assigned to one of 2 groups. One group was only insonated (US). The other group was insonated after the Kupffer cells phagocytized the ultrasound contrast agent (CEUS). Each group was divided into 4 subgroups according to intensity of insonation as follows MI 0.2 ($n=8$), 0.6 ($n=8$), 1.6 ($n=8$), and control ($n=6$).

Determination of HSP

The expression of HSP70 was determined to evaluate the cell-stress tolerance. We performed Western blot analysis after insonation as follows : whole cell lysates containing 20 μg of protein boiled in equal volumes of loading buffer protein were separated electrophoretically

Table 1 Grouping Phagocytosis of ultrasound contrast

Group	US				CEUS			
Subgroup	Control	MI 0.2	MI 0.6	MI 1.6	Control	MI 0.2	MI 0.6	MI 1.6
Sonazoid	−	−	−	−	+	+	+	+
US intensity*	−	0.2	0.6	1.6	−	0.2	0.6	1.6
Animal#	6	8	8	8	6	8	8	8

*: MI (mechanical index)

on 4–12% Tris-glycine gradient gels and subsequently transferred to pure nitrocellulose membranes (BOI-RAD) which were blocked with 5% nonfat dried milk in TBS for 2 hours. Primary antibody against Rabbit Anti−HSP70 polyclonal antibody (CSA-400 Stressgen Bioreagent, Canada) was applied at 1/1,000 dilutions overnight, followed by washing three times with TBS containing 0.05% Tween 20, secondary antibody IgG : HRP horseradish peroxidase conjugate adsorbed with human IgG (SAB-300, C) was applied at 1/10,000 dilution for 2 hours those blots were washed in TTBS three times and incubated for 10 minutes. Amersham ECL Western blotting detection reagents and analysis system (GE Healthcare, UK) and Versa Doc imaging system model 5,000, Nippon Laboratories (BPC-300) bio-rad super signal exposed to photographic film. Anti-β-Actin HSP70 Protein Active HSP70 HeLa Cell Lysate (Stressgen Bioreagent, Canada) was used as an internal control.

Determination of LDH

LDH leakage was determined to evaluate cell injury. After insonation quantitative analysis of the concentration of LDH in media was performed by Cytotoxicity Detection Kit PLUS (Roche Diagnostics GmbH, Germany).

Statistics

For statistical evaluation, student paired t-test was used to compare the data of HSP and LDH (software : SPSS ver. 16). A p-value less than 0.05 was considered to indicate a statistically significant difference.

Results

Microscopic observation

The results of microscopic observations were just described because all cases showed same phenomenon.

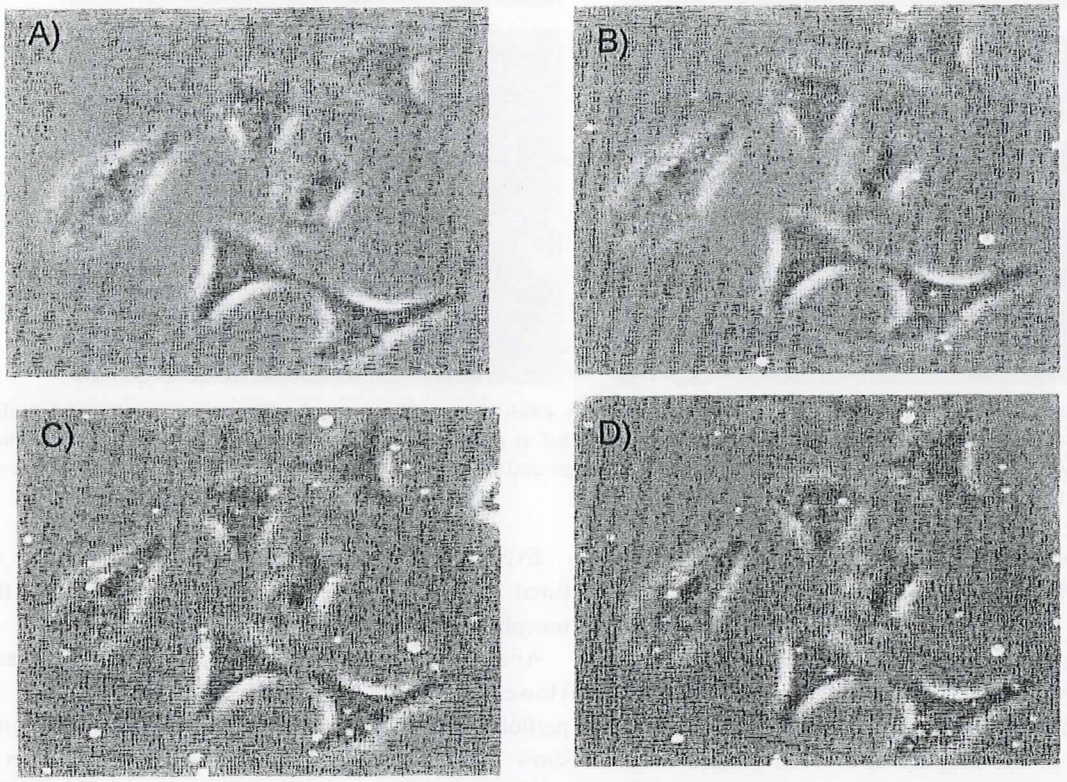

Fig. 1 Representative microscopic images under microscopy with 400-fold magnification. A) Before injecting microbubble solution, B) 30 seconds after, C) 15 minutes after, and D) 30 minutes after the injection. It appeared that all Kupffer cells completed phagocytizafion within 30 minutes.

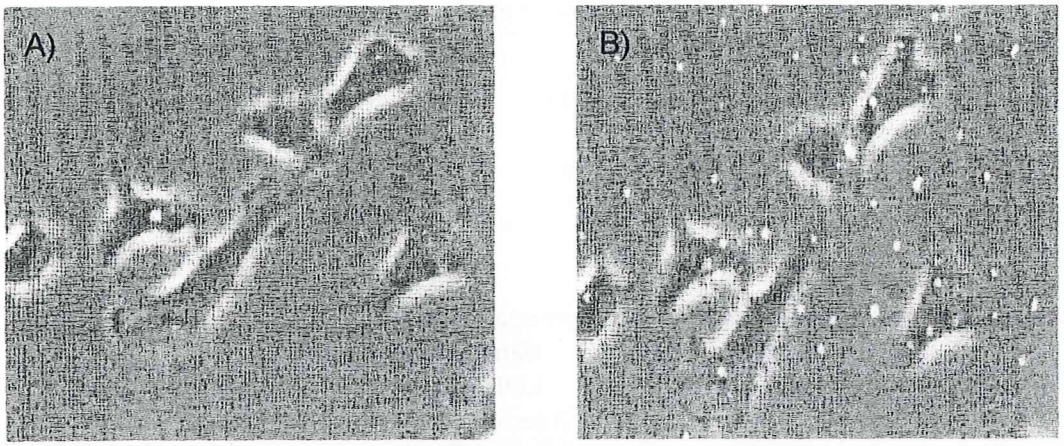

Fig. 2 Representative microscopic images under microscopy with 400-fold magnification. Before A), and after B) phagocytizing the perflubutane bubbles. The primary cultured Kupffer cells 24 hours after phagocytizing the perflubutane bubbles returned their shape as did the bubbles, under phase-contrast microscopy.

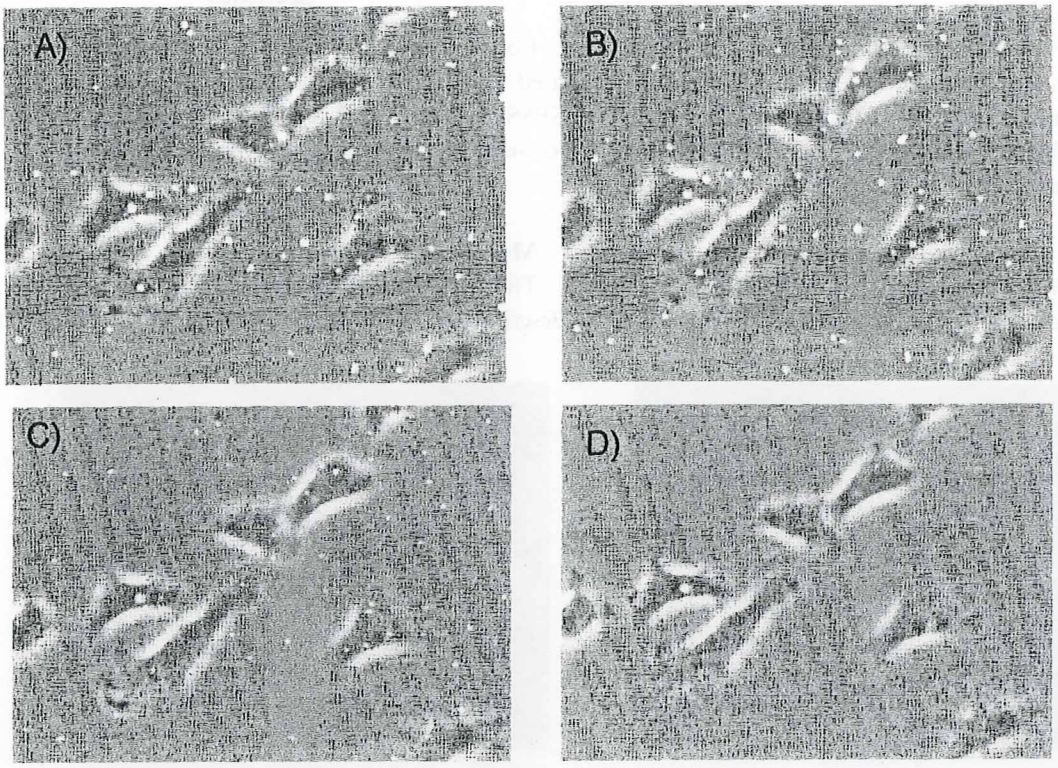

Fig. 3 Representative microscopic images under microscopy with 400-fold magnification. A) The primary cultured Kupffer cells 24 hours after phagocytizing the perflubutane bubbles before insonation. B) After insonation at MI 0.2. C) After insonation at MI 0.6, the shrunk free bubbles were desfroget and disappeared. D) After insonation at MI 1.6, most of the bubbles were not detectable.

The adhesion of the ultrasound contrast agent microbubbles to the Kupffer cells was completed within 30 seconds after filling with perflubutane. All cells phagocytized one to eight microbubbles within forty minutes. In the fastest case about 10 minutes after the adhesion, the microbubbles moved to the area adjacent to the nucleus of the Kupffer cells. All phagocytized microbubbles retained their shape. All Kupffer cells phagocytizing the microbubbles olso maintained their morphology.

Even 24 hours after phagocytization the primary cultured Kupffer cells and the microbubbles retaind their morphological appearance.

After insonation at MI 0.2 no change was detected. However, after insonation at MI 0.6, the free perflubutane bubbles in the culture solution began to show oscillation and some of them shrank. After insonation at MI 1.6, most of the free and phagocytized bubbles were fragmented or vanished and the leaked gas from the destroyed agents' shell agglutinated. On the

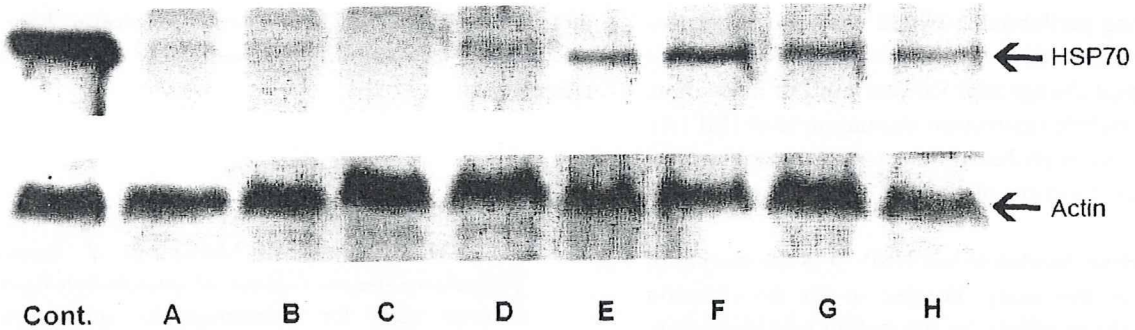

Fig. 4 Western blot of the revelation of HSP70 and β-Actin analyses.
A. blank. B. only insonation at MI 0.2. C. only insonation at MI 0.6. D. only insonation at MI 1.6. E. perflubutane. F. phagocytosis and insonation at MI 0.2. G. phagocytosis and insonation at MI 0.6. H. phagocytosis and insonation at MI 1.6 As for β-Actin loading control.

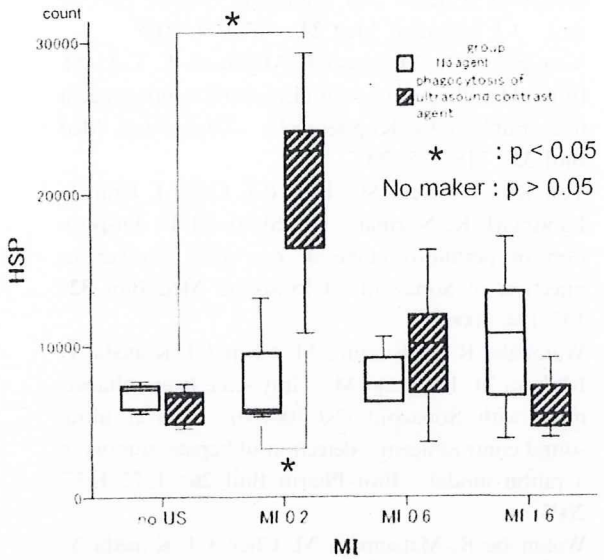

Fig. 5 Changes in the HSP expression
No significant change was observed within the US only groups, however in the CEUS only groups, the expression significantly increased at MI 0.2 ($p<0.05$) compared with control. Intergroup comparison at the same ultrasound intensity level the expression of the group of CEUS was significantly higher ($p<0.05$) especially at MI 0.2.

other hand, Kupffer cells were morphologically stable in all groups.

The analysis of the expression of HSP70

The β-Actin lines show the loading control. Analysis showed no significant change in the lines of β-Actin. No significant change in the expression of HSP70 was observed within the US group, however in the CEUS group, the expression significantly decreased with increase of MI ($p<0.05$). Intergroup comparison at same ultrasound intensity level especially at MI 0.2 showed significantly higher expression of HSP70 in the CEUS group than other groups ($p<0.05$). HSP70 expression of the controls of both groups shows no significant change.

The concentration of LDH

No significant increase in LDH concentration was detected in any group or subgroup.

Discussion

We set out to determine whether phagocytosis of ultrasound contrast agents and diagnostic low intensity insonation affects cell function.

The Kupffer cell is a macrophage in the liver. They naturally phagocytize the microbubbles of perflubutane and the phagocytized bubbles even react under insonation. Hepatocellular carcinoma (HCC) lesions are not enhanced by the ultrasound contrast agent in delayed phase images on clinical ultrasound contrast enhanced examination. The lesions have few Kupffer cells[3-5]. Therefore lesions of HCC should appear as hypoechoic areas compaired to bright noncancerous lesion. This effect remarkably improves screening for detection of HCC[6] lesions.

However a previous report suggested might that it should make adverse effects on liver cells[2].

In our study, to conform as much as possible to the situation of the insonated Kupffer cells during ordinary clinical ultrasound examinations, we employed the same, clinically used ultrasound contrast agent and diagnostic ultrasound equipment and probe as used in the clinical studies. However microenvironments surrounding Kupffer cells like serum, oxygen saturation, and other kinds of liver cells natarally differed from the in vivo situation, because they were isolated. It is undeniable that the differences could affect ultrasound attenuation and cell damage. However the experimental condition was able to evaluate responses from only Kupffer cells and to achieve a homogeneous insonation dose distribution.

The microscopic observation showed the stability of the perflubutane microbubble and the low interaction between the microbubbles and Kupffer cells. The phagocytizing Kupffer cells showed no morphological change for at least 24 hours. This result showed that

phagocytizing perflubutane would cause no acute toxicity for Kupffer cells. Moreover the cells showed no morphological change after various levels of insonation, even at the bubble destruction insonation level (MI 1.6).

HSP 70 accomplishes a key role to maintain the physiological function of the cell after many kinds of stress[7-9].

We therefore decided to use HSP 70 as the marker of cell stress in this study, because so far no common marker for the bioeffects for insonation with microbubble ultrasound contrast agents has been estabilised.

Interestingly, in the group of insonation with phagocytizing perflubutane, the expression of HSP 70 declined as the insonation intensity increase. On the other hand the insonation-only group showed no significant change. A paper by Nollen and Morimoto stated that in non-stress conditions HSP would bind with heat shock factor and be inactivated, and that immediately after stress, HSP would be released and activated[9]. It was assumed that US alone causes no stress for cells. If it did cause cell damage, the HSP expression would increase at higher insonation levels.

However it is a fact that low intensity insonation with phagocytizing perflubutane enhances some bioeffects. More intriguingly, low ultrasound intensity was more stressful for microbubble-phagocytized cells than high ultrasound intensity.

In next step we would like to make sure the interesting phenomenon. If just enhances the expression of HSP and causes no cell damage, preconditioning of insonation after phagocytizing the microbubbles of ultrasound contrast agent could reduce the adverse effects of liver ischemia-reperfusion injury resulting from partial hepatectomy[10][11]. In short, it is possible that a hepatic induced HSP level could induce higher hepatic cell-tolerance.

LDH is known as a stable enzyme contained in the cytoplasm of all cells and released promptly when the cell membrane is damaged[12]. This is the reason that LDH was selected as a marker of cell injury in this study. However no case showed elevation of LDH level. Even insonation with phagocytizing perflubutane seems to cause no irreparable harm which is compatible with the results of previous studyies[13][14]. However another report showed the microbubble burst of another ultrasound contrast agent at the surface of cell membrane under insonation causing perforations penetrating holes in just microseconds[15]. In our study most bubbles were inside the cell. This difference should decrease deleterious the harmful effects.

Conclusion

This study showed insonation after the Kupffer cells phagocytosed the ultrasound contrast agent caused no morphologic change of Kupffer cell. However there is an undeniable possibility that cell-stress could be increased.

References

1) Watanabe R, Matsumura M, Munemasa T, Fujimaki M, Suematsu M: Mechanism of hepatic parenchyma-specific contrast of microbubble-based contrast agent for ultrasonography: microscopic studies in rat liver. Invest Radiol **42**: 643-651, 2007

2) Shigeta K, Itoh K, Ookawara S, Taniguchi N, Omoto K: The effects of Levovist and DD-723 in activating platelets and damaging hepatic cells of rats. J Ultrasound Med **24**: 967-974, 2005

3) Yanagisawa K, Moriyasu F, Miyahara T, Yuki M, Iijima H: Phagocytosis of ultrasound contrast agent microbubbles by Kupffer cells. Ultrasound Med Biol **33**: 318-325, 2007

4) Toft KG, Hustvedt SO, Hals PA, Oulie I, Uran S, Landmark K, Normann PT, Skotland T: Disposition of perfluorobutane in rats after intravenous injection of Sonazoid. Ultrasound Med Biol **32**: 107-114, 2006

5) Watanabe R, Matsumura M, Chen CJ, Kaneda Y, Ishihara M, Fujimaki M: Gray-scale liver enhancement with Sonazoid (NC100100), a novel ultrasound contrast agent: detection of hepatic tumors in a rabbit model. Biol Pharm Bull **26**: 1272-1277, 2003

6) Watanabe R, Matsumura M, Chen CJ, Kaneda Y, Fujimaki M: Characterization of tumor imaging with microbubble-based ultrasound contrast agent, Sonazoid, in rabbit liver. Biol Pharm Bull **28**: 972-977, 2005

7) Andoh H, Itoh H, Koyama K, Sato Y, Tashima Y: Heat shock protein 70 in rat liver with necrosis and regeneration induced by thioacetamide. J Gastroenterol **29**: 293-298, 1994

8) Mikami K, Otaka M, Goto T, Miura K, Ohshima S, Yoneyama K, Lin JG, Watanabe D, Segawa D, Kataoka E, Odashima M, Watanabe S: Induction of a 72-kDa heat shock protein and protection against lipopolysaccharide-induced liver injury in cirrhotic rats. J Gastroenterol Hepatol **19**: 884-890, 2004

9) Ellen A, Nollen EA, Morimoto RI. Chaperoning signaling pathways: molecular chaperones as stress-sensing 'heat shock' proteins. J Cell Sci **115**: 2809-2816, 2002

10) Kume M, Yamamoto Y, Saad S, Gomi T, Kimoto S, Shimabukuro T, Yagi T, Nakagami M, Takada Y, Morimoto T, Yamaoka Y: Ischemic preconditioning of the liver in rats: implications of heat shock protein induction to increase tolerance of ischemia-reperfusion injury. J Lab Clin Med **128**:

251-258, 1996
11) Yamagami K, Yamamoto Y, Kume M, Kimoto S, Yamamoto H, Ozaki N, Yamamoto M, Shimahara Y, Toyokuni S, Yamaoka Y : Heat shock preconditioning ameliorates liver injury following normothermic ischemia-reperfusion in steatotic rat livers. J Surg Res **79** : 47-53, 1998
12) Orrenius S, Thor H, Rajs J, Berggren M : Isolated rat hepatocytes as an experimental tool in the study of cell injury. Effect of anoxia. Forensic Sci **8** : 255-263, 1976
13) Lindner JR, Dayton PA, Coggins MP, Ley K, Song J, Ferrara K, Kaul S : Noninvasive imaging of inflammation by ultrasound detection of phagocytosed microbubbles. Circulation **102** : 531-538, 2000
14) Kindberg GM, Tolleshaug H, Roos N, Skotland T : Hepatic clearance of Sonazoid perfluorobutane microbubbles by Kupffer cells does not reduce the ability of liver to phagocytose or degrade albumin microspheres. Cell Tissue Res **312** : 49-54, 2003
15) Goertz DE, Cherin E, Needles A, Karshafian R, Brown AS, Burns PN, Foster FS : High frequency nonlinear B-scan imaging of microbubble contrast agents. IEEE Trans Ultrason Ferroelectr Freq Control **52** : 65-79, 2005

Kupffer 細胞による超音波造影剤 perflubutane の取り込みと超音波照射による HSP70 の発現誘導作用について

木尼熱 熱夏提　廣川富彦　劉 広健
森安史典

東京医科大学内科学第四講座

目的：びまん性肝疾患、肝腫瘤性病変に対する画像診断に、造影超音波検査は検出感度が高い低侵襲性検査方法である。SONAZOID 造影超音波では、Kupffer 細胞内に取り込まれた造影剤が超音波照射を受けて、反射、共振、崩壊することで画像が得られる。これらの造影剤の変化による刺激が Kupffer 細胞内の HSP70 発現にどのような影響を及ぼすのかについて検討した。方法：雄性 Wistar ラット 18 週 60 匹を超音波と造影超音波 2 群に分け、さらに各群は音圧により、コントロール ($n=6$)、MI 0.2 ($n=8$)、0.6 ($n=8$)、1.6 ($n=8$) の 4 グループ (計 8 グループ) に分けて実験を行なった。肝組織より分離し、48 時間培養後の Kupffer 細胞の培養液中に、造影剤溶液を加えて気泡の貪食を顕微鏡で観察した。Kupffer 細胞がマイクロバブルを貪食したこと確認した後、Toshiba Aplio XV 造影モードで、30 秒照射し、細胞を 24 時間培養後、細胞を剥がして Western blot analysis HSP の誘導を検討した。結果：いずれの条件においても HSP の誘導が確認された。超音波のみ照射群では音圧の増加に連れて増加し MI 1.6 においてピークとなった。MI 1.6 においてコントロールと比べて有意な HSP の産生亢進を認めた。perflubutane＋超音波群において、MI 0.2 においてコントロールと比べて HSP の産生は著しく有意に亢進したが、音圧の増加に連れて低下し MI 1.6 では有意差がみられなかった。ピークは MI 0.2 の時点であった ($p<0.05$)。

超音波のみ照射群と perflubutane＋超音波群の同一音圧時の比較では、MI 0.2 の場合にのみ HSP の産生は perflubutane＋超音波群で有意に亢進しており、その他の音圧では有意差を認めなかった。結論：今回の実験から造影剤を Kupffer 細胞に貪食させた状況で臨床検査レベルの音圧の超音波を照射しても致死的な細胞傷害は認められない。しかし MI 0.2 より高い音圧レベルでは細胞の機能を何らかの形で障害しているおそれがある。

〈キーワード〉 Kupffer 細胞、HSP、perflubutane、超音波

特集

Step up MRI 2009

—前進！革新！MRI—

企画協力：吉川宏起　駒澤大学医療健康科学部教授

Step up MRI 2009

I MR造影剤の最新動向

1. Gd-EOB-DTPAのその後の評価

吉村　宜高／齋藤　和博／高良　憲一／長谷川大輔
柿崎　　大／徳植　公一　東京医科大学放射線医学講座
荒木　洋一／勝山　宏章／佐々木一良　東京医科大学放射線部
杉本　勝俊／目時　　亮／森安　史典　東京医科大学内科学第四講座

Gd-EOB-DTPA（EOB・プリモビスト：バイエル薬品）は，国内初の肝細胞特異性を有するMR造影剤である。ダイナミックスタディによる血流診断が可能な上，肝細胞造影相と呼ばれる投与後20分以降での遅延相で，肝細胞に特異的に取り込まれ，腫瘍検出能を向上させる。発売後1年半が経過し，その有用性や問題点が報告されてきている。

本稿では，当院における撮像法と工夫，そして主な対象疾患である肝細胞がん（hepatocellular carcinoma：HCC）を中心にその有用性や問題点について概説する。

当院でのEOB・プリモビスト造影MRIの撮像法と工夫

当院では，シーメンス社製1.5T MRI「MAGNETOM Avanto」を使用している。また，1年ほど前から32chボディアレイコイルを使用し，空間分解能の向上，さらには時間分解能の向上を得ている。EOB・プリモビスト造影MRIにおいては，検査時間の短縮が重要な課題であったが，現在当院では，造影剤投与後にT2強調像，拡散強調画像を撮像することにより，撮像時間の短縮を図っている[1]。われわれの初期の検討では，造影後にT2強調像や拡散強調画像を撮像しても，HCCの診断に関しては影響が少ないことを確認している（図1）。

撮像の手順は，単純MRIのT1強調像のin-phaseおよびopposed-phaseを撮像した後，直ちにダイナミックスタディを行い，肝細胞造影相を撮像するまでの間にT2強調像，拡散強調画像を撮像している。ダイナミックスタディおよび肝細胞造影相は，空間分解能に優れ

〈0913-8919/09/¥300/ 論文 /JCOPY〉

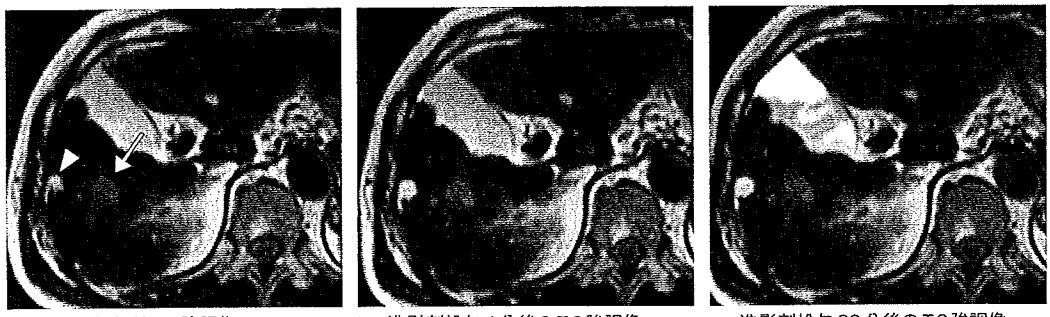

a：造影剤投与前T2強調像　b：造影剤投与4分後のT2強調像　c：造影剤投与20分後のT2強調像

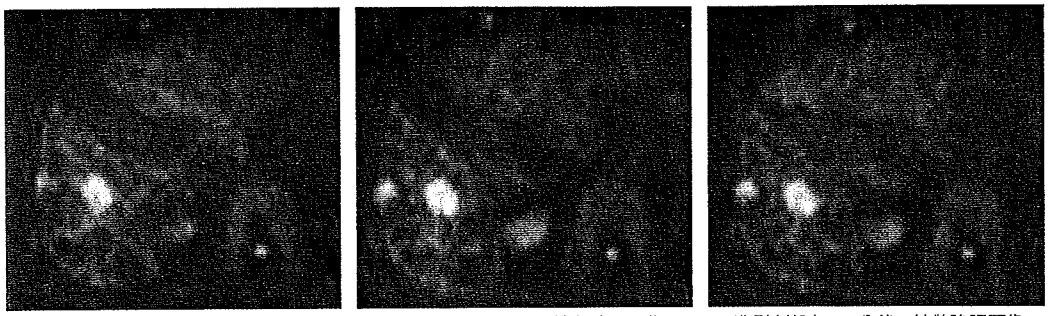

d：造影剤投与前の拡散強調画像 ($b=800 s/mm^2$)　e：造影剤投与4分後の拡散強調画像　f：造影剤投与20分後の拡散強調画像

図1　造影剤によるT2強調像，拡散強調画像への影響
HCCのコントラストは造影剤投与による影響が少ない。
▽：血管腫　⇩：HCC

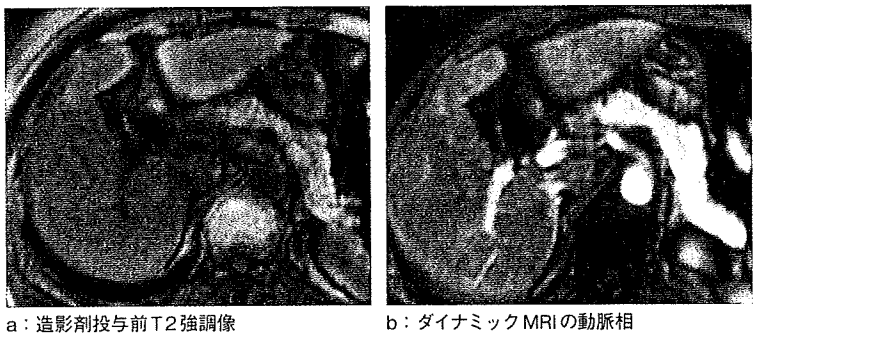

a：造影剤投与前T2強調像　b：ダイナミックMRIの動脈相

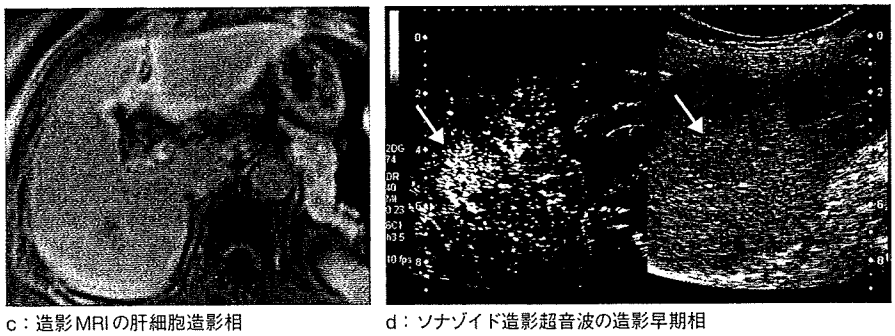

c：造影MRIの肝細胞造影相　d：ソナゾイド造影超音波の造影早期相

図2　ダイナミックMRIの動脈相で濃染が指摘できなかったHCC症例
造影MRIの肝細胞造影相(c)で，腫瘍は低信号に描出されている。ダイナミックMRIの動脈相(b)では多血性HCCとは診断困難である。しかし，ソナゾイド造影超音波の造影早期相(d)で腫瘍の染影が認められ，多血性HCCと診断された。

るthree-dimensional Volumetric Interpolated Breath-hold Examination (3D-VIBE) で撮像している。

ダイナミックスタディはボーラストラッキング法を使用して撮像しているが，32chボディアレイコイルが使用可能となってからは，画質を落とすことなくdouble arterial phaseを撮像することが可能となった。これにより安定した動脈相が得られるようになったが，適切なタイミングで撮像されていても非特異的細胞外液性造影剤と比較すると，造影効果は弱い印象を受ける。造影剤は2mL/sで注入し，生理食塩水40mLで後押しを行っている。生理食塩水は3mL/sで注入している。造影剤を3mL/s以上で高速注入すると，ringing artifactが生じる可能性が指摘されており[2]，注入速度は，ある程度のボーラス性を保つ必要があることからも2mL/sとしている。撮像開始時間は，大動脈遠位弓部に造影剤が達したことを確認してから9秒後にスキャンを開始している。当院での撮像機種では，k-space充填法はシーケンシャルオーダであり，動脈相の1相目のk-space中心が，大動脈遠位弓部に造影剤が到達してから11秒後に来るように撮像している。単純MRIで結節が高信号を示し，造影効果が評価困難な症例あるいはvascularityの評価が困難な症例には，ペルフルブタン（ソナゾイド：第一三共）を用いた造影超音波で血流診断を行っている（図2）。

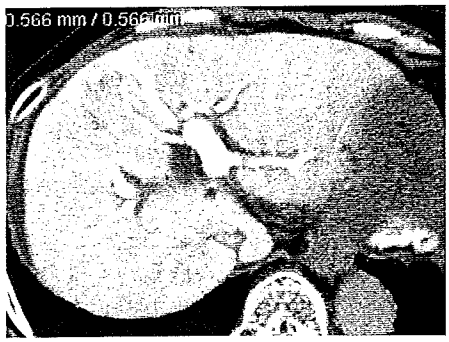

a：CTAP

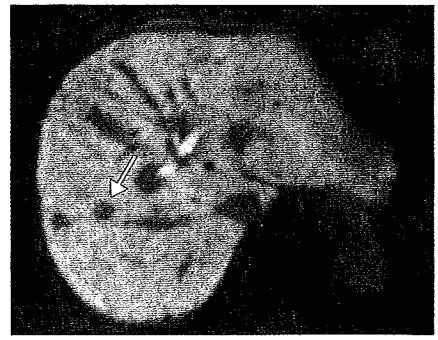

b：EOB・プリモビスト造影MRIの肝細胞造影相

図3　高分化型肝細胞癌
CTAP (a) では腫瘍は同定できない。EOB・プリモビスト造影MRIの肝細胞造影相 (b) では，低信号腫瘤が認められる（⇩）。生検の結果，高分化型肝細胞癌であった。その外側にも同様な腫瘤が認められる。生検は施行していないが，高分化型肝細胞癌が疑われる。

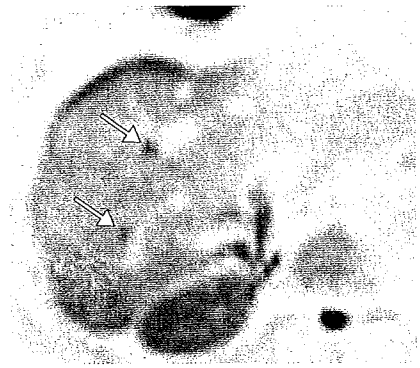

a：拡散強調画像（b＝800s/mm²）

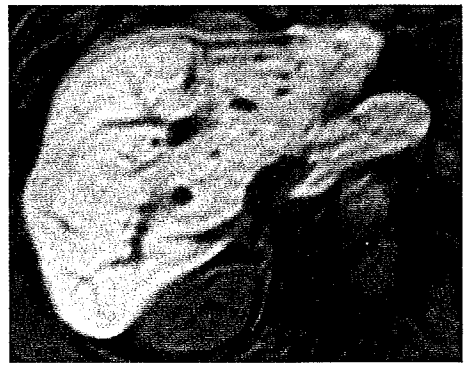

b：EOB・プリモビスト造影MRIの肝細胞造影相

図4　カルチノイドの肝転移
拡散強調画像 (a) では小さな転移性腫瘍が同定可能である（⇩）。EOB・プリモビスト造影MRIの肝細胞造影相 (b) では，血管との区別がつきにくく，同定しにくい。

肝腫瘍におけるEOB・プリモビスト造影MRIの有用性と問題点

1. 肝細胞がん（HCC）

HCCの診断に関して，最近の報告では経静脈性造影CTとの比較検討で，1cm以下の結節の診断に優れるとしている[3]。本造影剤は多血性のみならず，乏血性HCCの検出も非常に良好であり，検出能は血管造影下CTとほぼ同程度と考えている。われわれの経験では，血管造影下CTで同定が可能な結節は，ほとんど肝細胞造影相で検出可能であった。また，血管造影下CTで門脈血流が保たれ，肝細胞造影相で同定された結節はHCCの可能性が高いという結果を得ている（図3）。このような結節は早期HCCと考えられ[4]，一般的に悪性度は低く，施設によっては経過観察されていた病変である。今後，EOB・プリモビストが広く使用されるに従い，発見される機会が増加するものと考えられる。このような結節をどのように扱っていくかは今後，議論されることと思われる。

一方，肝細胞造影相で低信号とならず，高信号を示すHCCもあるので注意が必要である。高信号の原因としては，organic anion transporter（OATP）1Bの関与が報告されており，胆汁産生，分化度との関連性は低いとされている[5]。このようなHCCは，限局性結節性過形成などの良性病変との鑑別が重要となってくる。

2. 転移性肝腫瘍

転移性肝腫瘍の検出能は優れており，単純MRI，造影CTと比較して良好と報告されている[6]。また，超常磁性酸化鉄製剤（SPIO製剤）との比較では同等か，やや高い診断能を有すると報告されている[7]。しかし，SPIO製剤同様，小さなものは脈管との区別がつきにくく，病変の検出には拡散強調画像の併用が有効である（図4）。拡散強調画像を併用しないと，小病変を見逃す恐れがあるものと考えている。

◎

EOB・プリモビストがわが国で使用可能となってから1年半が経過した。わが国ではHCCを中心に新たな知見が報告され，ますますその有用性は高まっていくものと考えられる。

●参考文献
1) Zech, C.J., Herrmann, K.A., Reiser, M.F., et al. : MR imaging in patients with suspected liver metastases ; Value of liver-specific contrast agent Gd-EOB-DTPA. *Magn. Reson. Med. Sci.*, **6**, 43～52, 2007.
2) Carroll, T.J., Korosec, F.R., Swan, J.S., et al. : The effect of injection rate on time-resolved contrast-enhanced peripheral MRA. *J. Magn. Reson. Imaging*, **14**, 401～410, 2001.
3) Kim, S.H., Kim, S.H., Lee, J., et al. : Gadoxetic acid-enhanced MRI versus triple-phase MDCT for the preoperative detection of hepatocellular carcinoma. *Am. J. Roentgenol.*, **192**, 1675～1681, 2009.
4) Kojiro, M. : Focus on dysplastic nodules and early hepatocellular carcinoma : An Eastern point of view. *Liver Transplant*, **2**, S3～S8, 2004.
5) Narita, M., Hatano, E., Arizono, S., et al. : Expression of OATP1B3 determines uptake of Gd-EOB-DTPA in hepatocellular carcinoma. *J. Gastroenterol.*, 2009(in press).
6) Hammerstingl, R., Huppertz, A., Breuer, J., et al. : Diagnostic efficacy of gadoxetic acid (Primovist)-enhanced MRI and spiral CT for a therapeutic strategy ; Comparison with intraoperative and histopathologic findings in focal liver lesions. *Eur. Radiol.*, **18**, 457～467, 2008.
7) Kim, Y.K., Lee, Y.H., Kwak, H.S., et al. : Detection of liver metastases ; Gadoxetic acid-enhanced three-dimensional MR imaging versus ferucarbotran-enhanced MR imaging. *Eur. J. Radiol.*, 2009(in press).

東京医科大学消化器内科における APLIOによる肝腫瘤性病変のソナゾイド造影超音波

東京医科大学消化器内科
今井康晴、佐野隆友、村嶋英学、宮田祐樹、市村茂輝、平良淳一、
目時　亮、古市好宏、山田昌彦、中村郁夫、森安史典

はじめに

2007年1月、次世代超音波造影剤であるソナゾイドが世界に先駆けて本邦で発売され、肝疾患における造影超音波検査の役割が高まりつつある[1]。ソナゾイドの撮像方法は超音波装置ごとに推奨される方法が示されてはいるものの、背景肝疾患、病変部位、病変のエコーレベルなどにより撮像条件の調整が必要である。また、Mechanical index(以下 M.I.)は装置ごと・撮像モードごとにより特性があるため、ソナゾイド投与量、M.I.は装置間・撮像モード間での単純な比較は困難である。今回、我々が日常行っている東芝メディカルシステムズ社製APLIOによるソナゾイド造影超音波の撮像条件を示す。

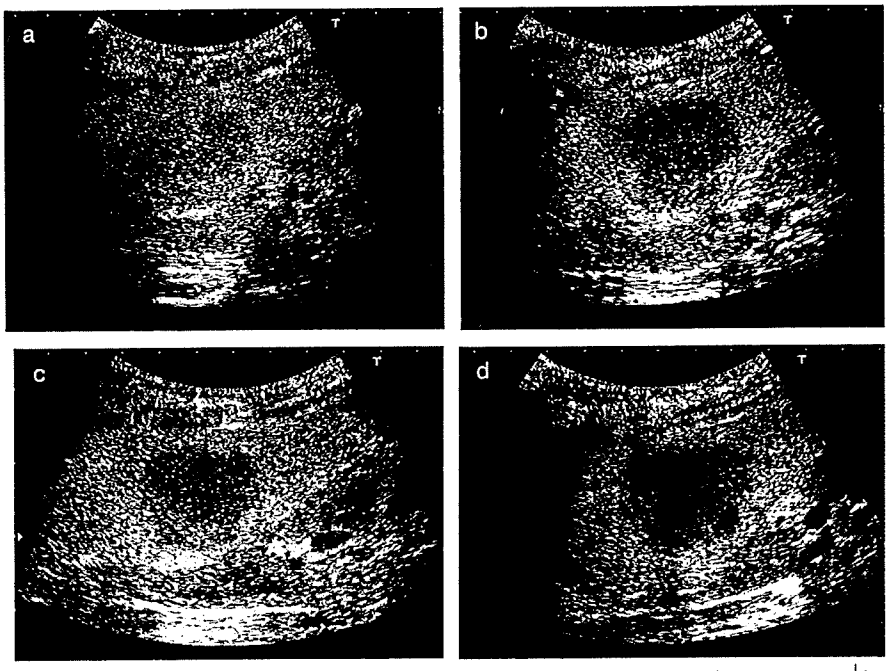

図1　Kupffer相の撮像タイミング
ソナゾイド投与10分後(a)、20分後(b)、30分後(c)、60分後(d)と、時間の経過とともに腫瘍部位の造影欠損が明瞭となってきている。

対象

対象は、2007年1月から2009年3月までの間、肝腫瘤性病変に対して東芝メディカルシステムズ社製APLIOによるソナゾイド造影超音波を行った、延べ1,485例(肝細胞癌 836例、転移性肝腫瘍147例、肝血管腫93例、限局性結節性過形成15例、肝膿瘍22例、その他372例)である。

撮像条件

超音波装置は、東芝メディカルシステムズ社製APLIO XV、APLIO XGを用い、Pulse subtraction low MI mode(PS low)またはDifferential CHI low MI mode(D-CHI)で撮像した。ソナゾイドの投与量は0.5～1.0mL/bodyを肘静脈より急速静注した。撮像条件は、原則としてMechanical index 0.15～0.30、Frame rate 15fps前後、Dynamic range 35～50dBとし、Gain、STCは画像が均一になるように適宜調整した。Focusは1点focusとして、focus位置をDynamic studyで腫瘍下縁、Micro flow imaging(MFI)[2]で腫瘍中心、Kupffer相で視野下縁を原則とした。Kupffer相の撮像はソナゾイド投与後10分間以上とした。Kupffer相の10分後に造影欠損が明瞭でない場合は20分後まで待って観察するが、臨床的には8分後で病変部が周囲肝より明らかに低エコーとなっている場

合は造影低下と判断して良いと考える(図1)。PS lowにおけるソナゾイドの投与量は、Dynamic study、MFIで0.5mL/body、Kupffer相で処置する場合は0.5～1.0mL/bodyとした。当科での経験では、体重別に投与量を調節しなくても画像はほとんど変わらなかった。一方、D-CHIではソナゾイドの振動により得られる映像の他に、ソナゾイドの破壊による映像も加わっている[3]ため、ソナゾイド投与量に関してDynamic studyではPS lowより少なくてもよく、Kupffer相で処置する場合はPS lowと同じか、やや多めがよいと考えられる。

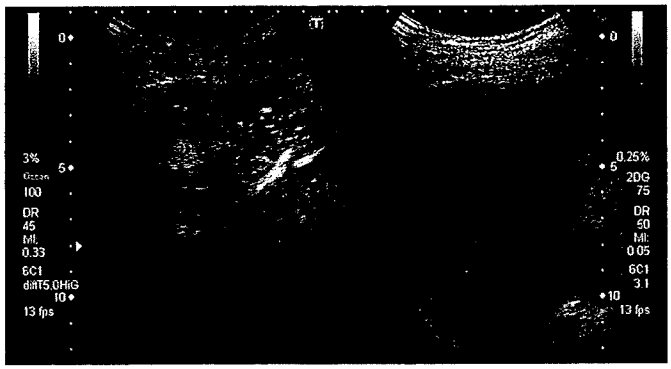

図2　脂肪肝を伴った肝硬変症例
脂肪肝、肝硬変の症例では、Differential CHI low MI mode(D-CHI)でM.I.をやや高めにすると造影性が良くなることがある。本症例では、D-CHI、M.I.は0.33にて撮像した。

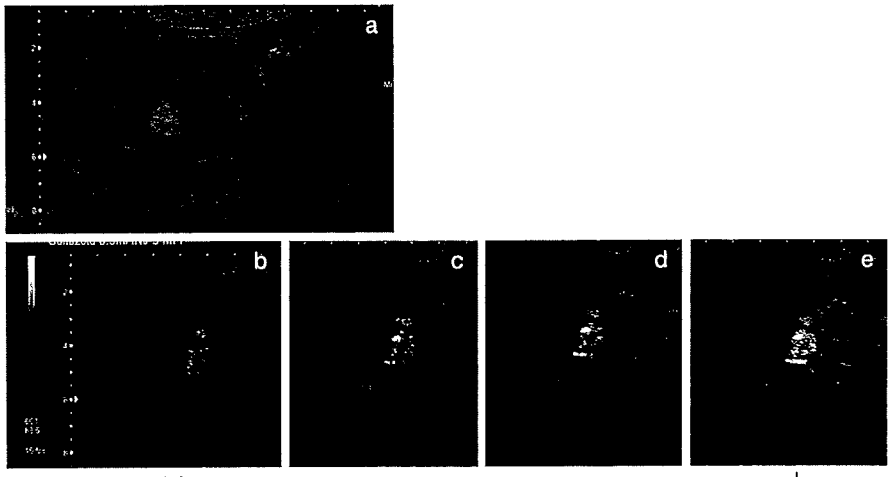

図3　高エコー腫瘤のMicro flow imaging
高エコー腫瘤(a)では、Micro flow imaging(MFI)で病変のエコーレベルが徐々に上昇してくることでも造影されていることがわかる(b、c、d、e)。

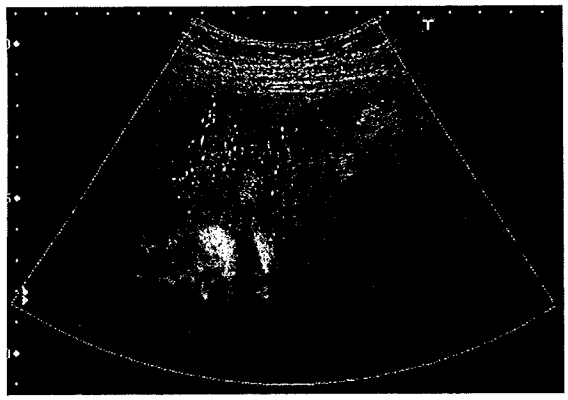

図4　高エコー腫瘤のKupffer相
高エコー腫瘤のKupffer相では、レボビストの造影モードであるAdvanced Dynamic Flow(ADF)が有用のことがある。

症例

症例1：脂肪肝を伴った肝硬変症例

脂肪肝、肝硬変の症例では、造影モードの画像にすると、病変がわかりにくくなることがある。そのような場合は、低音圧基本波の画像をモニターとして腫瘍の位置をリアルタイムに確認しながら造影を行う。また、図2の症例のようにD-CHIでM.I.をやや高めにすると造影性が良くなることがある。

症例2：高エコー腫瘤

高エコー腫瘤の場合は、病変をやや拡大して描出し、GAINを暗めに調節して造影を行う。高エコーのため腫瘤内への造影剤の流入がわかりにくいが、高エコーの部分にバブルが動いているのが観察されることで造影されているのがわかる。さらに、MFIで病変のエコーレベルが徐々に上昇してくることでも造影されていることがわかる(図3)。また、低音圧造影モードによるKupffer相での診断は、組織の高エコーと造影の高エコーの区別がつかなくなるため判定が非常に困難となる。このような場合は、高音圧で、しかも造影画像と基本画像の分離が可能であるレボビストの造影モードAdvanced Dynamic Flow(ADF)が有用である(図4)。

おわりに

当科におけるAPLIOによる肝腫瘤性病変に対するソナゾイド造影超音波の撮像方法を示した。今後、さらに良好な画像が安定して得られる撮像方法の開発が期待される。

<文献>
1) 今井康晴ほか: 一般医のためのエコー活用法 造影エコー. Medicina 44: 391-395, 2007
2) 西田　睦ほか: 頸部リンパ節微細血管描出のための新しい造影US法. Jpn J Med Ultrasonics 31: J347-J353, 2004
3) 鈴木陽一ほか: 映像技術. 超音波造影ガイドブック(森安史典ほか). 金原出版: 21-27, 2003

Pediatr Surg Int (2009) 25:1017–1020
DOI 10.1007/s00383-009-2457-0

CASE REPORT

Complete resection of hepatoblastoma originating in the caudate lobe: case report and literature review

Hiroyuki Koga · Yoichi Ishizaki · Junya Fujimura · Tadaharu Okazaki · Naho Fujiwara · Geoffrey J. Lane · Toshiaki Shimizu · Atsuyuki Yamataka · Seiji Kawasaki

Published online: 21 August 2009

Abstract Hepatoblastoma originating in the caudate lobe is extremely rare, and resection is technically challenging. The aim of this study was to report our experience of complete resection of hepatoblastoma originating in the caudate lobe and review the literature. A 12-month-old boy was admitted for investigation of an upper abdominal mass. Imaging studies showed an irregularly lobulated 8-cm solid tumor in the left lobe of the liver. Serum α-fetoprotein was 67,700 ng/mL. This tumor was diagnosed as hepatoblastoma (PRETEXT II) and chemotherapy (3 courses of CDDP and ADR) was performed. After chemotherapy, the tumor had shrunk to a resectable size and its origin in the caudate lobe could be determined. Left hepatic lobectomy with en bloc resection of the caudate lobe was performed. Total blood loss was 10 mL, and the operation lasted 9 h. His postoperative course was uneventful. Preoperative chemotherapy facilitated complete resection by left hepatic lobectomy with total excision of the caudate lobe.

This paper was presented at the 46th Japanese Society of Pediatric Surgeons Meeting, 1–3 June 2009 in Osaka, Japan.

H. Koga · T. Okazaki (✉) · N. Fujiwara · G. J. Lane · A. Yamataka
Department of Pediatric General and Urogenital Surgery, Juntendo University School of Medicine, Tokyo 113-8421, Japan
e-mail: okazakit@juntendo.ac.jp

Y. Ishizaki · S. Kawasaki
Department of Hepatobiliary-Pancreatic Surgery, Juntendo University School of Medicine, Tokyo, Japan

J. Fujimura · T. Shimizu
Department of Pediatrics, Juntendo University School of Medicine, Tokyo, Japan

Keywords Hepatoblastoma · Caudate lobe · Complete resection

Introduction

Hepatoblastoma is the most common primary hepatic malignant tumor in childhood. Tumor arising from the caudate lobe has been rarely reported [1–3].

In this paper, we present our case and review the literature about complete resection of hepatoblastoma originating in the caudate lobe.

Case report

A 12-month-old boy presented to our institution with upper abdominal distention. Upon admission, ultrasonography showed a huge mass occupying almost the entire left hepatic lobe. Computed tomography (CT) was performed and identified a single low-density mass 8 cm in diameter preferentially located in the left hepatic lobe, with no evidence of tumor thrombi in the portal vein or intrahepatic metastases (Fig. 1a). Serum-alpha-fetoprotein (AFP) was 67,700 ng/mL. These findings led to a diagnosis of hepatoblastoma originating in the left hepatic lobe (PRETEXT II) [4]. The patient had preoperative chemotherapy consisting of cisplatin (80 mg/m^2) and adriamycin (30 mg/m^2). After completion of three 4-week courses, AFP decreased to 105 ng/mL, and on CT the diameter of tumor decreased to 3 cm. Although the precise origin of the tumor had not been identified before chemotherapy, we were now able to determine that it originated in the caudate lobe (Fig. 1b).

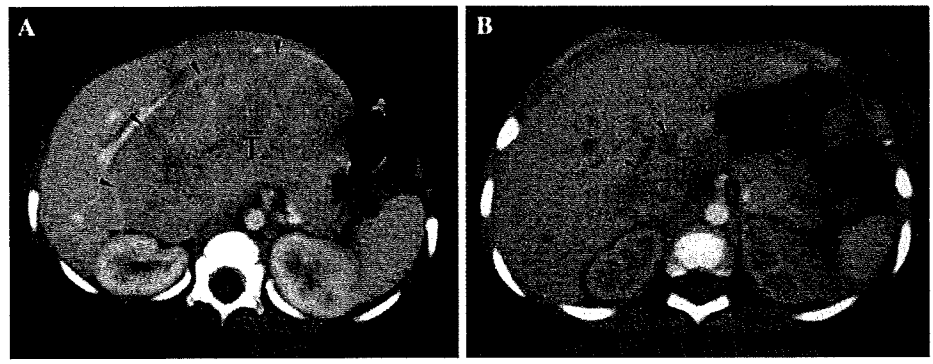

Fig. 1 **a** Before chemotherapy, a huge tumor (*T* surrounded by *arrowheads*) measuring 8 cm is seen occupying almost the entire left lobe. **b** After preoperative chemotherapy consisting of cisplatin and adriamycin, CT reveals the tumor (*T* surrounded by *arrowheads*) has decreased to 3 cm

Although the caudate lobe can be excised easily by extended left lobectomy with dissection of the hepatic middle vein, in this case, CT angiography showed that the right anterior lateral segment (S6) drained only through the middle hepatic vein (Fig. 2); so we planned a left lobectomy with en bloc resection of the caudate lobe to preserve the middle hepatic vein.

An abdominal approach through bilateral subcostal with midline upward incisions was chosen to expose a wider surgical field. On opening the lesser omentum, the caudate lobe was seen to be replaced by tumor (Fig. 3a); intraoperative ultrasonography demonstrated that the inferior vena cava (IVC) was patent. First, we isolated the caudate lobe from the IVC with great care taken to divide the short hepatic vain. After the left hepatic artery and the portal vein had been divided, the demarcation line between both lobes could be seen clearly. In the parenchyma, we divided the liver along the middle hepatic vein, which was preserved and exposed on the cut surface. The root of the left hepatic vein was ligated and divided in the parenchyma.

Fig. 2 CT angiography showing that the right anterior lateral segment (S6) drains only through the middle hepatic vein (*arrowheads*)

Thus, left lobectomy was achieved en bloc with resection of the entire caudate lobe (Fig. 3b). During the whole procedure, Pringle's vascular occlusion was used for 15 min and followed by 5 min of perfusion, which was repeated five times. Total blood loss was 10 mL, and the operation lasted 9 h.

Histopathologic examination revealed a hepatoblastoma of fetal type. Surgical margins were negative for tumor. Postoperative chemotherapy consisting of cisplatin and adriamycin was commenced on the 12th day. After two 4-week courses, AFP levels decreased below the normal limit in a linear manner. This patient is still doing well 12 months after surgery, without any signs of recurrence.

Discussion

The caudate lobe is generally divided into three regions: the left Spiegel, the process portion, and the paracaval portion. Branches of the portal vein and bile ductules are distributed in each of these portions [5]. Caudate lobectomy may be performed when the tumor is limited to either the left caudate lobe or the caudate process. However, resection of the caudate lobe often has been considered a technically challenging procedure, even to accomplished hepatic surgeons [6]. Surgical removal of the tumor in the caudate lobe is risky because the anatomy of the caudate lobe and its close proximity to major vascular structures make resection difficult, such as attached directly IVC, where the hepatic veins from the caudate lobe may be short-ended. During isolation and dissection of the blood supply and bile ducts to the tumor, the IVC may be easily damaged, causing fatal hemorrhage. The major problems in caudate lobe resection are in dissection and control of the retrohepatic caudate veins and anteriorly, in the presence of substantial tumor, in controlling bleeding from the middle hepatic vein. Thus, an associated left or right lobectomy must be done when the tumor originates from the paracaval portion or extended to the entire caudate lobe [1, 2]. The preferred side for lobectomy must be determined case by

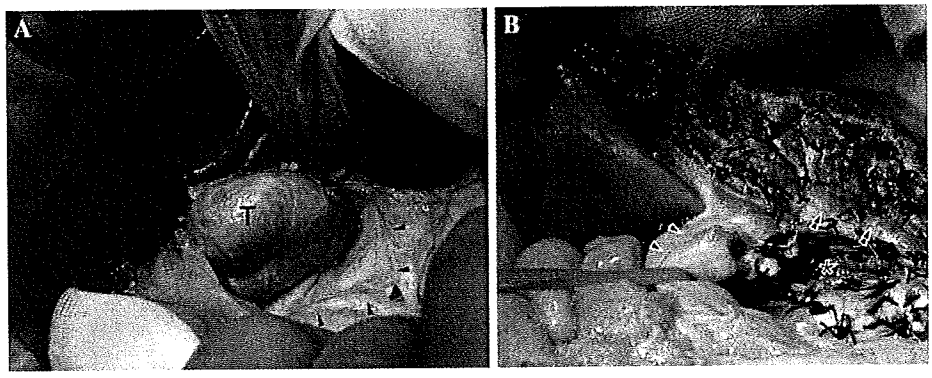

Fig. 3 **a** Gross appearance of the liver. The left side of the tumor (*T*) is seen through an opening in the lesser omentum (*arrowheads*). **b** Cut surface of the liver after left lobectomy with en bloc resection of the entire caudate lobe. The middle hepatic vein (*double arrowheads*) is exposed and the cavity (*asterisk*) where the tumor was located is seen behind the middle hepatic vein. *Arrowheads* show the common bile duct

Table 1 Clinical characteristics of children with hepatoblastoma originating in the caudate lobe in the literature [1–3]

Case	Year	Age (months)	Length of Op (min)	Blood loss (g)	Surgical procedure	Preoperative chemotherapy
Case 1 [1]	1990	4	280	36	LH with CL	+
Case 2 [2]	1991	60	–	–	Ex LH with CL and IVC resection	+
Case 3 [3]	1992	18	–	2,800	Isolated CL	–
Present case		12	540	10	LH with CL	+

LH Left hepatectomy, *Ex LH* extended left hepatectomy, *CL* caudate lobectomy, *IVC* inferior vena cava

case, taking into consideration the cranial extent of the tumor and the origin and dominance of feeder vessels. For example, the paracaval portion has been reported to derive blood from the transverse portion of the left portal branch in 74% and from the right in 26% [5].

The most recent approach in treating hepatoblastoma is to remove the tumor completely by using systemic chemotherapy and surgery. Despite improvements in surgical techniques and supportive care, complete primary resection is possible in less than 50% [7, 8]. Chemotherapy is able to shrink the size of a tumor as well as make it more defined and less friable allowing surgery to be safer with reduced blood loss. In our case, we were only able to identify the origin of the tumor as the caudate lobe after chemotherapy.

In the English literature there are only three other cases of hepatoblastoma arising in the caudate lobe [1–3] (Table 1). Two cases underwent combined extended left, and left lobectomy with en bloc resection of the caudate lobe, respectively, because preoperative chemotherapy was able to reduce the size of the tumor from occupying the entire left hepatic lobe, to show that it originated in the caudate lobe [1, 2]. However, in the other case, a left lobectomy was planned without preoperative chemotherapy because the surgeons diagnosed that there was no indication of the tumor originated in the caudate lobe [3]. They only noticed the actual origin of the tumor intraoperatively but injured the IVC resulting in massive fatal blood loss.

Essentially, surgery should be considered as novel resection technique, tend to be associated with a much high risk for incomplete tumor removal, as well as a greater chance for postoperative complications [9]. In our case, we detached the caudate lobe completely from the IVC at an early stage as recommended by Takayama et al. [1] and chose to combine left lobectomy with en bloc resection of the entire caudate lobe because the tumor was confined completely to the caudate lobe. Our case was young with excellent liver function. Young patients are able to tolerate up to 75–80% resections of the original liver mass because of excellent regenerative capabilities [10, 11], unlike adults who may be complicated by hepatitis and cirrhosis.

This case is the third case of hepatoblastoma originating in the caudate lobe, treated successfully and safely by resection after preoperative chemotherapy to decrease tumor size. Left lobectomy with en bloc resection of the caudate lobe was safe, effective, and gave excellent results.

References

1. Takayama T, Makuuchi M, Takayasu K, LeThai B, Ohyama H, Yamazaki S et al (1990) Resection after intraarterial chemotherapy of a hepatoblastoma originating in the caudate lobe. Surgery 107:231–235
2. Takayama T, Makuuchi M, Kosuge T, Yamazaki S, Hasegawa H, Takayama J et al (1991) A hepatoblastoma originating in the caudate lobe radically resected with the inferior vena cava. Surgery 109:208–213
3. Okada A, Yoneda A, Azuma T, Yagi M, Fukuzuwa M, Kamata S (1992) A resected case of hepatoblastoma originating in the caudate lobe. Eur J Pediatr Surg 2:49–51
4. Roebuck DJ, Aronson D, Clapuyt P, Czauderna P, de Goyet J, Gauthier F et al (2007) 2005 PRETEXT: a revised staging system for primary malignant liver tumours of childhood developed by the SIOPEL group. Pediatr Radiol 37:123–132
5. Kumon M (1985) Cast preparations of the liver and their clinical application Branches of the portal vein and bile ducts in the caudate lobe. Acta Hepatologica Japonica 26:1193–1199
6. Sarmiento JM, Que FG, Nagorney DM (2002) Surgical outcomes of isolated caudate lobe resection: a single series of 19 patients. Surgery 132:697–709
7. Czauderna P, Otte JB, Roebuck DJ, von Schweinitz D, Plaschkes J (2006) Surgical treatment of hepatoblastoma in children. Pediatr Radiol 36:187–191
8. Tiao GM, Bobey N, Allen S, Nieves N, Alonso M, Bucuvalas J et al (2005) The current management of hepatoblastoma: a combination of chemotherapy, conventional resection, and liver transplantation. J Pediatr 146:204–211
9. Fuchs J, Rydzynski J, Hecker H, Mildenberger H, Burger D, Harms D et al (2002) The influence of preoperative chemotherapy and surgical technique in the treatment of hepatoblastoma—a report from the German Cooperative Liver Tumour Studies HB 89 and HB 94. Eur J Pediatr Surg 12:255–261
10. Howard ER, Stringer MD, Colombani PM (2002) Surgery of the liver bile ducts and pancreas in children. EdardArnold, New York, pp 219–237
11. Stringer MD, Oldham KT, Mouriquand PDE (2006) Pediatric surgery and urology long-term outcomes, 2nd edn. Cambridge University Press, Cambridge, pp 799–814